

RESEARCH ARTICLE

Structural changes of erythrocyte membrane revealed by 3D confocal optical profilometer

Tatiana A. Lomanovskaya¹  | Gennadii A. Piavchenko¹  |
 Vladislav O. Soldatov²  | Artem A. Venediktov¹  | Egor A. Kuzmin¹  |
 Natalia L. Kartashkina¹  | Svetlana G. Mukhamedova¹  |
 Tatiana V. Boronikhina¹  | Aleksandr G. Markov¹  | Dmitry V. Telyshev^{1,3}  |
 Igor Meglinski^{4,5}  | Alexander N. Yatskovskiy¹ 

¹Department of Histology, Cytology and Embryology, I.M. Sechenov First Moscow State Medical University (Sechenov University), Moscow, Russia

²Pharmacology and Clinical Pharmacology Department, Belgorod National Research University, Belgorod, Russia

³Institute of Biomedical Systems, National Research University of Electronic Technology, Zelenograd, Moscow, Russia

⁴Opto-Electronics and Measurement Techniques, Faculty of Information and Electrical Engineering, University of Oulu, Oulu, Finland

⁵College of Engineering and Physical Sciences, Aston University, Birmingham, UK

Correspondence

Gennadii A. Piavchenko, Department of Histology, Cytology and Embryology, I.M. Sechenov First Moscow State Medical University (Sechenov University), Mokhovaya Str., 11/10, Moscow 125009, Russia.

Email: gennadii.piavchenko@staff.sechenov.ru

Igor Meglinski, College of Engineering and Physical Sciences, Aston University, Birmingham B4 7ET, UK.

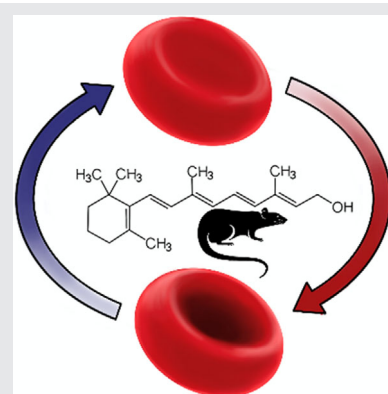
Email: i.meglinski@aston.ac.uk

Funding information

Academy of Finland, Grant/Award Numbers: 325097, 351068; Leverhulme Trust and The Royal Society, Grant/Award Number: APX111232; The Ministry of Science and Higher Education of the Russian Federation, Grant/Award Number: 075-15-2022-304

Abstract

We examined hematological changes influenced by the experimental hypervitaminosis A. The 3D confocal optical profilometer was applied for assessment of the erythrocytes' membrane structural changes influenced by an overdose of vitamin A. The blood smears were evaluated in terms of alterations of geometrical and optical parameters of erythrocytes for two groups of animals: oil base and retinol palmitate (n = 9 animals for each group). The results demonstrate that an overdose of retinol palmitate causes changes in the torus curvature and pallor of discocytes, their surface area and volume. The observed structural malformations of the shape of red blood cells become visible at the earlier preclinical stage of changes in animal state and behavior. With this in mind, the results of the study open a new area of research in the certain dysfunction diagnosis of red blood cells and have a great potential in the further development of new curative protocols.



Tatiana A. Lomanovskaya and Gennadii A. Piavchenko are same impact authors.

This is an open access article under the terms of the [Creative Commons Attribution-NonCommercial-NoDerivs](https://creativecommons.org/licenses/by-nc-nd/4.0/) License, which permits use and distribution in any medium, provided the original work is properly cited, the use is non-commercial and no modifications or adaptations are made.

© 2022 The Authors. *Journal of Biophotonics* published by Wiley-VCH GmbH.

KEYWORDS

3D confocal optical profilometry, erythrocyte morphology, hypervitaminosis A, morphodensitometric traits, retinol palmitate

1 | INTRODUCTION

The elevated lability of biochemical, physicochemical and morphological red blood cells (RBC) parameters is widely used for a membranotropic xenobiotics toxicity screening of, that is, for drugs toxicity [1, 2]. RBC aggregation, membrane deformability, shape and form-factor parameters of erythrocytes can reflect the alterations of hemorheological properties of RBC induced by nanomaterials and substances [3–5]. The results of these studies clearly show actual morphological alterations of the RBC membrane caused by nanoparticles and nano-based substances exposure. Nevertheless, testing of the biocompatibility of nanomaterials and substances with RBC is challenging due to complex interaction matter, which depends on concentration, local density, size, composition, geometry, surface properties and properties of biological surrounding. Transported through the blood circulation system nano-substances are interacting with blood components, especially with RBC, comprised 40% to 45% of blood. At normal conditions, the form of RBC is changed dramatically upon interaction with nanomaterials [3–8]. Impairment of morphodensitometric traits such as membrane integrity, morphology, deformability and aggregation induced by an overdose of a nano-substance can lead to microrheology alterations and result in thrombosis [9–11]. Here, we explore how the overdose of vitamin A influences the RBC structure.

Vitamin A (retinol) and its analogues demonstrate lipophilic and membranotropic features that allow to use it as drugs [12]. However, biologically active forms of vitamin A are reported to demonstrate a dose-dependent toxicity [13] resulting in restrictions of their clinical use. Various literature reviews inform about cases of acute and chronic retinol toxicity both in humans and in animals. It affects various organs and systems, especially the skin, digestive tract, muscles, bones, nervous system, liver, spleen and peripheral blood as well. In the peripheral blood, one can find a drop of RBC osmotic resistance and of hemoglobinemia, an increase of poikilocytes number, as well as hemolysis and anemias [14–16]. Moreover, retinol in high doses can negatively impact cells and tissues even before clinical signs of hypervitaminosis A emerge [17]. It is highly required to find methodical approaches to predict a subtoxic state development. RBC seems to be the most appropriate object for a such study since they are easy to obtain from humans and experimental animals. Additionally, the cells have similar reactions to the action of various pathogenic factors. Initial

biochemical plasmalemma rearrangements lead to a shift of its viscoelastic properties and to a drop of the ability to be reversibly deformed. Thus, it results in morphological features of the cells [18]. Therefore, administering retinol medications and recording erythrocytes morphological changes in response to the treatment, one may take advantage of the resulting dose-dependent toxicity to define prognostic criteria for hypervitaminosis A.

The RBC of mammals is typically shaped as biconcave disks. This feature is unique and allows them to be very elastic and their deformation is usually reversible. Due to this fact, RBC passes easily through narrow capillaries and walls of the splenic venous sinuses. These properties are provided by the RBC plasmalemma and by the cytoskeleton which is attached to the membrane via compound macromolecular complexes. The cytoskeleton lays under the plasmalemma cytoplasmic surface in a form of a flexible reticular structure [19, 20]. The RBC plasmalemma is in fact the only structural component of the highly differentiated cells, which participates in all the processes of their functioning (due to the absence of the nucleus and other organelles). The erythrocytic membrane works as a selective permeability barrier that is crucial for intracellular homeostasis and RBC volume. It is also a key structure for the gas metabolism because of carrying out the most important RBC function, that is, the transportation of O₂ and CO₂. The membrane assists in the energetic metabolism via forming of structural and functional bonds with glycolytic enzymes. It also has a great number of surface receptors, and takes part in the transporting of various substances: hormones, enzymes, regulatory peptides, nucleotides and drugs as well [19–21].

The aforementioned distinctions of the RBC plasmalemma make it highly sensitive to any disorder of blood homeostasis. It results as an issue in different systemic diseases, for example, arterial hypertension, ischemic heart disease, diabetes, nephropathies, hepatitis, alcoholism, malignant tumors and autoimmune pathologies. Therefore, we may find chemical composition changes of the RBC plasmalemma, a peroxide oxidation increase, water-electrolyte balance disorders of the cytoplasm, a drop of the membrane elasticity and deformability, a growth of the poikilocytes number (echinocytes, spherocytes and stomatocytes), a higher cell sensitivity to hemolysis and finally, an eryptosis activation. In severe cases there may occur such complications as a clinically significant anemia and microcirculatory derangements that aggravate the course of the disease [22–26]. The analysis of RBC membrane properties may be carried out with various approaches.

High-resolution images of erythrocyte membrane may be obtained via atomic force microscopy [27], blood flow parameters—via automated rheoscope [28], cellular interactions and manipulations—with an application of optical tweezers and other techniques [8, 29]. All these methods allow to assess different RBC properties that may be useful in blood flow diagnostics and experiments on a single or a group of cells, but the most appropriate method for our goals is the morphodensitometry of RBC membrane structure using optical profiler.

In this article, we present the analysis of experimental hypervitaminosis A effect on the structural properties of erythrocyte membrane in rats.

2 | MATERIALS AND METHODS

3D models of erythrocytes and initial measurements were carried out on Sensofar S Neox 090 3D Confocal Optical Profiler in confocal mode (Sensofar-Tech, Spain)—Figure 1. Using hardware & software system “DiaMorph Cito” (CJSC “Diamorp,” Russia) we have processed digitized images of the blood smears measuring geometrical and optical parameters for erythrocytes (discocytes). 3D Confocal Optical Profilometry is a promising method that allows to assess surface features such as roughness, topography and

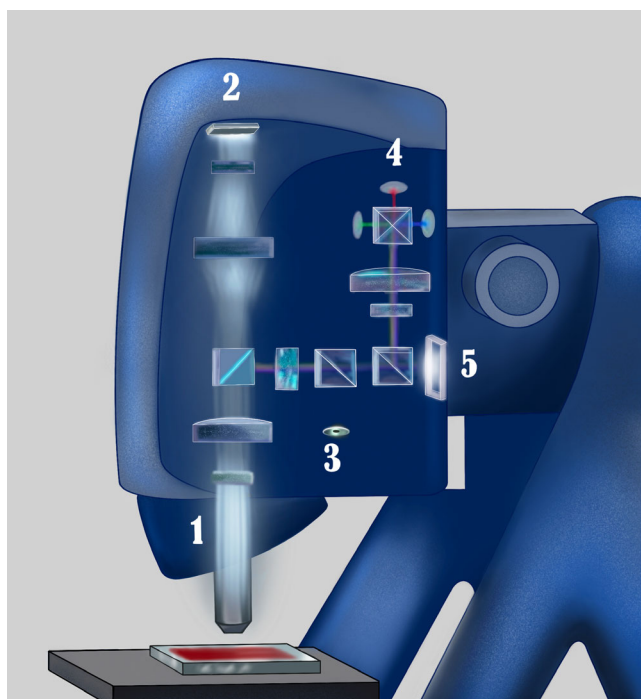


FIGURE 1 Sensofar S Neox 3D Confocal Optical Profiler (Sensofar-Tech, Spain) system scheme: 1—objective, 2—camera, 3 and 4—light sources, 5—microdisplay

flatness. In biomedicine, it gives the information of the cellular membrane and its structural properties.

This approach provided entire description of how morphological and functional features of RBCs have been changing. By this operation, we have quantitatively evaluated early signs and RBC response to the exposure. The measured parameters have included standard morphodensitometric variables [30, 31]. Among them, we have considered following: the area of discocyte projection onto a plane (top view); the area of its pallor (the concave central region of cytoplasm); the ratio of the two mentioned parameters; finally, the integrated optical density of cytoplasm. We have also examined some parameters of discocytes side view: the curvature of torus (convex peripheral ring in discocyte) upward and downward parts; the pallor curvature; the surface area; the volume; also, the ratio of both the last variables. The data of the morphodensitometric analysis have been used to provide a computer reconstruction of three-dimensional discocytes images.

An optical filter with a peak transmission in the range from $\lambda = 530$ nm to $\lambda = 580$ nm has been exploited to increase the contrast of the digitized images. The morphodensitometric parameters have been registered for 30 discocytes located in the adjacent fields of view from smear's central portion. The measurement has been conducted using blood smears of all the enrolled animals using a $50\times$ objective. When designing the experiment, we regarded individual and group parameter dispersion for discocytes of 10 intact rats. Then we calculated the sample size (the number of studied cells and the number of animals) assuming permissive error not to exceed 5%.

The statistical analysis of the obtained data has been carried out by IBM PASW Statistics 18.0.0. We have used non-parametric Mann–Whitney U test to evaluate the significance of differences in two samples' means. We also have chosen the confidence level of $P \leq .05$ to be critical.

The experiment has been carried out using 18 male Wistar rats which were obtained from branch “Stolbovaya” of the Federal State Budgetary Institution of Science “Scientific Center of Biomedical Technologies” of Russian Federal Medical & Biological Agency. The animals have been maintained and manipulated according to the rules of Good Laboratory Practice (the Russian Federation Ministry of Health Order #199n by 01/04/2016). After a week of adaptation to the vivarium conditions, the animals have been divided into two groups ($n = 9$ per group). The initial mean body mass of the rats has been equal to 120.9 ± 2.6 g. The body mass has not differed initially among each separate group ($P = .8$) with its further changes being recorded during the experiment. The study has been approved by the Ethical Committee of Sechenov University (protocol no 02-20 dated Feb 05, 2020).

In order to induce hypervitaminosis A, we have used oil-based retinol palmitate solution. The medication has been administered at a dose of 150 000 IU (0.3 mL of the solution) via gavage by a mouth soft feeding tube during 6 days. The control group received only vehicle (oilbase) in the same volume.

To make smears, we have taken a blood drop from a 2-mm-deep prick in the tail vein with a sterile scarifier. Then the prepared smears have been dried and fixed in methanol for 15 minutes. We have simultaneously stained the blood smears from experimental and control animals with Leishman stain solution (eosin and methylene blue).

3 | RESULTS AND DISCUSSION

The first signs of retinol palmitate overdose have been registered on the 5th day after the first administration. We have observed behavioral reactions changes, increased respiratory rate and body mass loss in the animals. The average model of erythrocyte size and form were calculated for the blood collected on the 6th day of experiment. The dynamics of body mass changes, models of

erythrocytes on the 6th day of experiment both for the experimental and for the control groups and representative images of measurements are shown in Figure 2.

The statistically significant ($P = .001$) differences of the variables between the groups have been revealed on the 5th and 6th day of the observation. The body mass of rats treated with retinol palmitate has been equal then to 87% (117/134) and to 80% (114/143), comparing with the control group.

Figure 3 represents how the morphodensitometric parameters' values of discocytes have been changing during the experiment. To wit, in retinol palmitate overdose the mean values of the area of discocyte projection onto a plane have not differed significantly between both groups during all the observation period (A). Meanwhile the integrated optical density of discocytes cytoplasm has been found to be strongly reduced on the same days. Even earlier than standard geometrical and optical cell parameters have changed (namely on the days 3 and 4), we have regarded the torus upward and downward parts curvature and there have revealed an increase of the mean values (B, C). The values of pallor curvature have diminished on the 6th day of retinol palmitate intake (D). In total, the change in curvature of different discocyte regions has

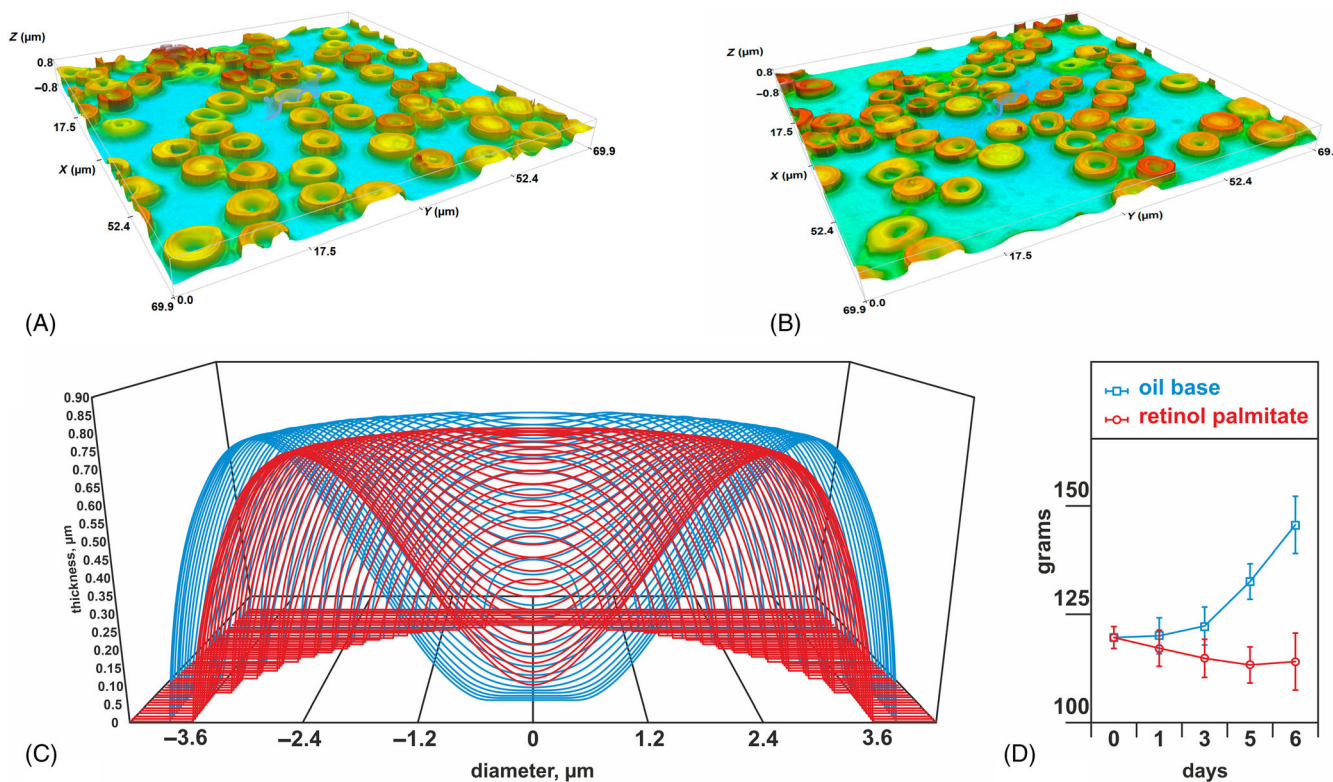
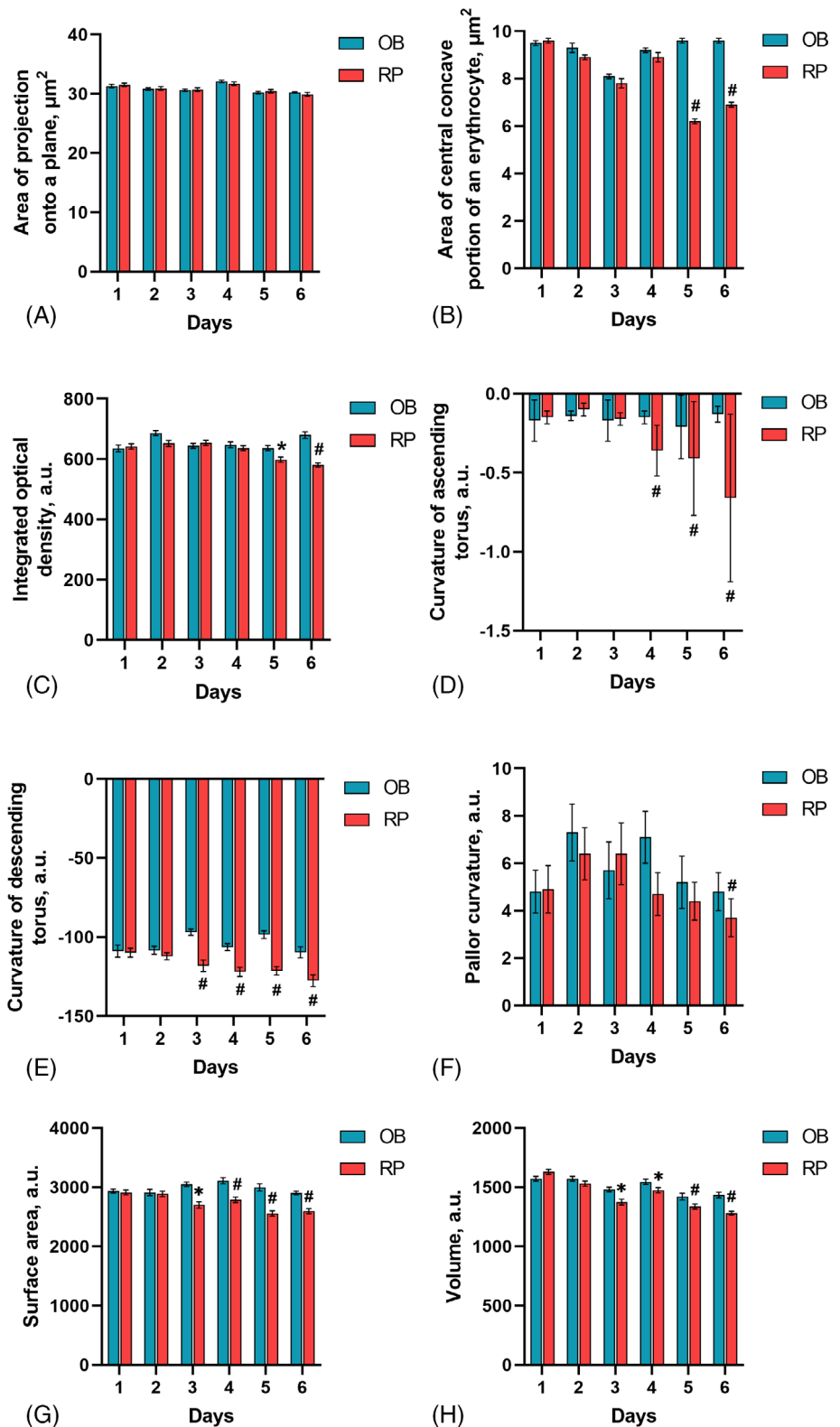


FIGURE 2 (A,B) Images of RBC on the day 6 of experiment for the retinol palmitate and oil base groups respectively, μm ; (C) reconstruction of an average discocyte three-dimensional image, μm . Blue is a control group and red is an experimental group. Day 6 of retinol palmitate administration; (D) the dynamics of rats' body mass changes for the both groups, g , $P = .001$

FIGURE 3 Dynamics of changes in morphodensitometric parameters (MDM) of rats' discocytes in retinol palmitate overdose ($\bar{X} \pm SD$). (A) Area of projection onto a plane; (B) area of central concave portion of an erythrocyte; (C) integrated optical density; (D) curvature of the ascending torus; (E) curvature of the descending torus; (F) pallor curvature; (G) surface area; (H) volume. OB—oil base (control group); 2—retinol palmitate (experimental group); * $P < .05$ in comparison to OB; # $P < .005$ in comparison to OB (Mann–Whitney U test)



resulted in a shift of their shape. The shift is easily seen at the reconstruction of three-dimensional images. Finally, the ratio between pallor and projection area (Figure 4A) and surface area and volume (Figure 4B), reflecting significantly decreased on the 5th and 6th day.

By the end of the experiment, the shape of discocytes obtained from rats treated with retinol palmitate has been reported to demonstrate a lower height of the torus region along with a pallor thickening despite a decrease in the pallor area. Notably, the curvature changes have

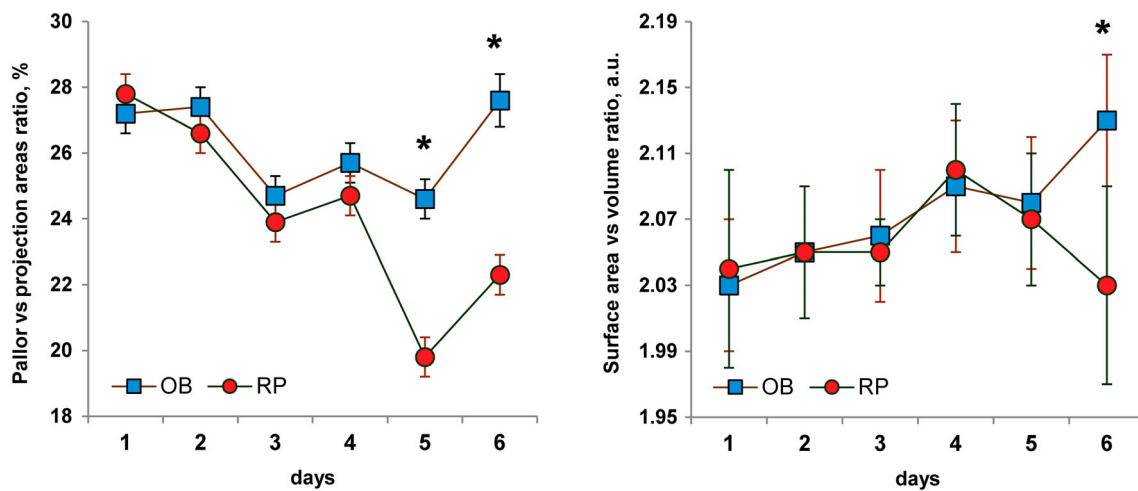


FIGURE 4 Graphs of ratio between pallor and projection area (A) and surface area and volume (B). Notable changes of RBC structure are most expressed in day 5 and 6. Other parameters are given in Figure 3

been accompanied by a decrease in their surface area and volume (since day 3). However, the ratio of these two last parameters has remained constant until the 6th day when it has significantly decreased (Figure 4).

Interestingly, the abovementioned changes of morphodensitometric parameters have been revealed in different days of observation. In particular, even before first signs of the overdose (3rd and 4th days) we have noted that the mean curvature values of upward and downward torus parts, as well as the mean surface area and the mean discocytes volume have become considerably different from those in the control group. Nevertheless, other parameters of discocytes changed simultaneously with the first clinical signs of hypervitaminosis A.

The dose of retinol palmitate chosen for the study was adequate to rapidly induce hypervitaminosis A in rats. Herein we show that morphological changes of RBC were detected before emergence of visible signs for retinol palmitate toxic effects (preclinical stage). The clinical course of hypervitaminosis was characterized by weight loss which is considered a one of the hallmarks in retinol overdose [14, 15]. After entering the body, retinol is stored in the liver in the form of esters, and then is transported to peripheral tissues being bound to retinol-binding protein [32]. In young rats, retinol circulates in the blood for a longer time than in adult ones [33]. Due to this fact, its content in the blood can be significantly higher. It is believed to be one of the reasons for more rapid development of hypervitaminosis A at a young age even if taking smaller doses of retinol [16]. The initial body mass of the enrolled rats corresponded to approximately 1.5 to 2 months of age [34], so the onset of hypervitaminosis A signs in 5 to 6 days after the start of the retinol palmitate administration has been surely provoked not only by the overdose but also by the animals age.

During all days of observation, the area of discocyte projection onto a plane (top view) has not significantly differed from that one in the control group. The parameter notwithstanding, other variables such as torus upward and downward parts curvature, the pallor curvature and area, finally, the ratio of the areas (the pallor area and the area of discocyte projection onto a plane) have evidenced a gradual change of the cells shape. We assume that this abnormality is associated with a modifying impact of retinol palmitate on RBC's membranes. In the presence of retinol, erythrocyte membrane viscoelasticity and fluidity change due to an increase in cholesterol [35] and phospholipids content, as well as because of redistribution of the phospholipids within lipid bilayer [36]. These phenomena affect an erythrocytic ability to undergo a reversible deformation [37].

In addition to the changes of viscoelastic features in the membrane, hemoglobin concentration also influences this ability of RBC to change their shape reversibly [38]. Decreased integrated optical density, a marker of hemoglobin concentration [39], indicates a lower hemoglobin content in retinol palmitate overdose. Notably, this change manifested simultaneously with hypervitaminosis A.

In erythrocytes, the surface area and its ratio to volume are criteria of deformation severity [30, 31]. The obtained data has revealed a decrease of both parameters in the discocytes of the experimental group rats since 3rd day of the experiment. Notably, the rates decrease for both surface area and volume have been identical in the discocytes as their ratio remained unchanged during almost all the observation period with a considerable decrease on the day 6 only. Thence we suppose that the observed erythrocytic deformation is not critical and seems to be reversible at the preclinical stage of hypervitaminosis A in retinol palmitate overdose.

We have especially remarked that the changes in morphodensitometric parameters of discocytes have been asynchronous in animals fed daily by retinol palmitate. Besides, the values of almost all measured parameters of discocytes in the experimental group animals have considerably changed exactly in the moment of overdose manifestation. In the absence of clinical signs, just few parameters (the curvature of torus upward and downward parts, the surface area and the volume) have differed significantly from the control group. It confirms data which were reported in literature describing toxic effects of retinol at the preclinical stage of hypervitaminosis A [17]. Moreover, we assume that these parameters may be used as prognostic criteria for retinol palmitate overdose.

4 | CONCLUSION

The detected changes of morphodensitometric parameters in discocytes are non-specific. Such changes could also arise due to various factors, but then they must show another direction and severity. That is why if one chooses RBC's as an object of morphodensitometric analysis then it is highly recommended to assess the nature of morphologic changes considering both acting factors and durations of their action when the prognostic criteria are determined for normal state and pathology.

This study has revealed special changes in RBC's morphology induced by retinol palmitate overdose. Notable, a big body of these changes was detected before clinical manifestation of hypervitaminosis A. Changes in the torus curvature and pallor of discocytes, their surface area can serve as markers of preclinical stage of retinol overdose. These traits may serve as important prognostic criteria for hypervitaminosis A development.

AUTHOR CONTRIBUTIONS

Tatiana A. Lomanovskaya: data curation, formal analysis, project administration, resources, software, writing—original draft. **Gennadii A. Piavchenko:** formal analysis, investigation, methodology, resources, writing—original draft. **Vladislav O. Soldatov:** formal analysis, critical review and editing. **Artem A. Venediktov:** visualization, writing—original draft. **Egor A. Kuzmin:** visualization, formal analysis. **Natalia L. Kartashkina:** conceptualization, project administration, visualization. **Svetlana G. Mukhamedova:** conceptualization, methodology, project administration, resources. **Tatiana V. Boronikhina:** conceptualization, formal analysis, funding acquisition, methodology, supervision, validation, writing—original draft. **Aleksandr G. Markov:** critical review and editing. **Dmitry V. Telyshev:** project administration, resources. **Igor Meglinski:** critical review

and editing. **Alexander N. Yatskovskiy:** conceptualization, data curation, formal analysis, investigation, methodology, project administration, resources, software, supervision, visualization, writing—original draft.

ACKNOWLEDGMENTS

Gennadii A. Piavchenko and Igor Meglinski acknowledge funding from the Academy of Finland (projects 325097 and 351068). This work was funded by the Ministry of Science and Higher Education of the Russian Federation within the framework of State support for the creation and development of World-Class Research Centers “Digital Biodesign and Personalized Healthcare” No. 075-15-2022-304 and partially funded by the Leverhulme Trust and The Royal Society (Ref. no.: APX111232 APEX Awards 2021). Tatiana A. Lomanovskaya and Gennadii A. Piavchenko contributed equally to this work. The authors acknowledge Mrs. Tatiana Koryashkina for her artwork in this article.

CONFLICT OF INTEREST

The authors declare no potential conflict of interests.

DATA AVAILABILITY STATEMENT

Research data are not shared.

ORCID

Tatiana A. Lomanovskaya  <https://orcid.org/0000-0001-7604-9415>

Gennadii A. Piavchenko  <https://orcid.org/0000-0001-7782-3468>

Vladislav O. Soldatov  <https://orcid.org/0000-0001-9706-0699>

Artem A. Venediktov  <https://orcid.org/0000-0002-5604-0461>

Egor A. Kuzmin  <https://orcid.org/0000-0003-4098-1125>

Natalia L. Kartashkina  <https://orcid.org/0000-0003-4648-9027>

Svetlana G. Mukhamedova  <https://orcid.org/0000-0001-6769-4543>

Tatiana V. Boronikhina  <https://orcid.org/0000-0001-9532-7898>

Aleksandr G. Markov  <https://orcid.org/0000-0002-3194-6064>

Dmitry V. Telyshev  <https://orcid.org/0000-0002-4221-9882>

Igor Meglinski  <https://orcid.org/0000-0002-7613-8191>

Alexander N. Yatskovskiy  <https://orcid.org/0000-0003-4387-7307>

REFERENCES

- [1] M. Farag, M. Alagawany, *Chem. Biol. Interact.* **2018**, 279, 73. <https://doi.org/10.1016/j.cbi.2017.11.007>.

- [2] M. Pagano, C. Faggio, *Cell Biochem. Funct.* **2015**, *33*, 351. <https://doi.org/10.1002/cbf.3135>.
- [3] T. Avsievich, Y. Tarakanchikova, R. Zhu, A. Popov, A. Bykov, I. Skovorodkin, S. Vainio, I. Meglinski, *Micromachines* **2020**, *11*, 19. <https://doi.org/10.3390/mi11010019>.
- [4] T. Avsievich, A. Popov, A. Bykov, I. Meglinski, *Sci. Rep.* **2019**, *9*, 5147. <https://doi.org/10.1038/s41598-019-41643-x>.
- [5] T. Avsievich, Y. Tarakanchikova, A. Popov, A. Karmenyan, A. Bykov, I. Meglinski, in *Novel Biophotonics Techniques and Applications V. Proc. SPIE*, Vol. 11075 (Eds: A. Amelink, S. K. Nadkarni), SPIE, Bellingham, WA **2019**, 110750F. <https://doi.org/10.1117/12.2526730>.
- [6] Y. Tian, Z. Tian, Y. Dong, X. Wang, L. Zhan, *RSC Adv.* **2021**, *11*, 6958. <https://doi.org/10.1039/D0RA10124A>.
- [7] R. Wadhwa, T. Aggarwal, N. Thapliyal, A. Kumar, Priya, P. Yadav, V. Kumari, B. S. C. Reddy, P. Chandra, P. K. Maurya, *3 Biotech* **2019**, *9*, 79. <https://doi.org/10.1007/s13205-019-1807-4>.
- [8] R. Zhu, T. Avsievich, A. Popov, A. Bykov, I. Meglinski, *Biosens. Bioelectron.* **2021**, *175*, 112845. <https://doi.org/10.1016/j.bios.2020.112845>.
- [9] Y. Bian, K. Kim, T. Ngo, I. Kim, O.-N. Bae, K.-M. Lim, J.-H. Chung, *Part. Fibre Toxicol.* **2019**, *16*(1), 9. <https://doi.org/10.1186/s12989-019-0292-6>.
- [10] M. J. Kim, S. Shin, *Food Chem. Toxicol.* **2014**, *67*, 80. <https://doi.org/10.1016/j.fct.2014.02.006>.
- [11] Z. He, J. Liu, L. Du, *Nanoscale* **2014**, *46*, 720. <https://doi.org/10.1039/c4nr01857e>.
- [12] M. R. De Oliveira, *Oxidat. Med. Cell. Longev.* **2015**, *2015*, 140267. <https://doi.org/10.1155/2015/140267>.
- [13] V. I. Nozdrin, Y. T. Volkov, *Retinoidy Alm.* **1995**, *2*, 12 (in Russian). <https://retinoids.ru/uploads/almanah2.pdf>.
- [14] O. M. Alarcón-Corredor, R. Alfonso, *Arch. Latinoam. Nutr.* **2007**, *57*, 224 (in Spanish). <https://pubmed.ncbi.nlm.nih.gov/18271400/>.
- [15] D. O. Edem, *Asian J. Clin. Nutr.* **2009**, *1*, 65.
- [16] K. L. Penniston, S. A. Tanumihardjo, *Am. J. Clin. Nutr.* **2006**, *83*, 191. <https://doi.org/10.1093/ajcn/83.2.191>.
- [17] P. M. Lind, S. Johansson, M. Rönn, H. Melhus, *Chem. Biol. Interact.* **2006**, *159*, 73. <https://doi.org/10.1016/j.cbi.2005.10.104>.
- [18] M. Chen, F. J. Boyle, *J. Biomech. Eng.* **2017**, *139*, 121009. <https://doi.org/10.1115/1.4037590>.
- [19] A. D. Nigra, C. H. Casale, V. S. Santander, *Cell. Mol. Life Sci.* **2020**, *77*, 1681. <https://doi.org/10.1007/s00018-019-03346-4>.
- [20] M. Trybus, L. Niemiec, A. Biernatowska, A. Hryniewicz-Jankowska, A. F. Sikorski, *Folia Histochem. Cytobiol.* **2019**, *57*, 43. <https://doi.org/10.5603/FHC.a2019.0007>.
- [21] R. J. Asaro, Q. Zhu, *Biomech. Model. Mechanobiol.* **2020**, *19*, 1361. <https://doi.org/10.1007/s10237-020-01302-x>.
- [22] R. Bissinger, A. A. M. Bhuyan, S. M. Qadri, F. Lang, *FEBS J.* **2019**, *286*, 826. <https://doi.org/10.1111/febs.14606>.
- [23] A. V. Hebbani, D. R. Vaddi, P. P. Dd, V. NCh, *J. Ayurveda Integr. Med.* **2021**, *12*, 330. <https://doi.org/10.1016/j.jaim.2021.02.001>.
- [24] E. Lang, R. Bissinger, S. M. Qadri, F. Lang, *Int. J. Cancer* **2017**, *141*, 1522. <https://doi.org/10.1002/ijc.30800>.
- [25] E. Pretorius, *Clin. Hemorheol. Microcirc.* **2018**, *69*, 545. <https://doi.org/10.3233/ch-189205>.
- [26] M. Zara, G. F. Guidetti, M. Camera, I. Canobbio, P. Amadio, M. Torti, E. Tremoli, S. S. Barbieri, *Int. J. Mol. Sci.* **2019**, *20*, 2840. <https://doi.org/10.3390/ijms20112840>.
- [27] I. Dulinska, M. Targosz, W. Strojny, M. Lekka, P. Czuba, W. Balwierz, M. Szymonski, *J. Biochem. Biophys. Methods* **2006**, *66*, 1. <https://doi.org/10.1016/j.jbbm.2005.11.003>.
- [28] A. Bransky, N. Korin, A. Leshansky, N. Lanir, Y. Nemirowski, U. Dinnar, *Rheol. Acta* **2007**, *46*, 621. <https://doi.org/10.1007/s00397-006-0146-7>.
- [29] T. Avsievich, R. Zhu, A. Popov, A. Bykov, I. Meglinski, *Rev. Phys.* **2020**, *5*, 100043. <https://doi.org/10.1016/j.revip.2020.100043>.
- [30] C. Renoux, M. Faivre, A. Bessaa, L. Da Costa, P. Joly, A. Gauthier, P. Connes, *Sci. Rep.* **2019**, *9*, 6771. <https://doi.org/10.1038/s41598-019-43200-y>.
- [31] H. Park, S. Lee, M. Ji, K. Kim, Y. Son, S. Jang, Y. Park, *Sci. Rep.* **2016**, *6*, 34257. <https://doi.org/10.1038/srep34257>.
- [32] D. N. D'Ambrosio, R. D. Clugston, W. S. Blaner, *Nutrients* **2011**, *3*, 63. <https://doi.org/10.3390/nu3010063>.
- [33] L. Tan, M. H. Green, A. C. Ross, *J. Nutr.* **2014**, *145*, 403. <https://doi.org/10.3945/jn.114.204065>.
- [34] A. N. Koterov, L. N. Ushenkova, E. S. Zubenkova, A. A. Wainson, A. P. Biryukov, A. S. Samoylov, *Med. Radiol. Radiat. Saf.* **2018**, *63*, 1 (in Russian). https://doi.org/10.12737/article_5ac6190e95da25.42157674.
- [35] I. Erturan, M. Naziroğlu, V. B. Akkaya, *Cell Biochem. Funct.* **2012**, *30*, 552. <https://doi.org/10.1002/cbf.2830>.
- [36] M. Abed, K. Alzoubi, F. Lang, A. Al Mamun Bhuayn, *Cell. Physiol. Biochem.* **2017**, *41*, 543. <https://doi.org/10.1159/000457014>.
- [37] A. Górnicki, *Int. J. Clin. Pharmacol. Ther.* **2006**, *44*, 648. <https://doi.org/10.5414/CP44648>.
- [38] N. L. Parrow, P. C. Violet, H. Tu, J. Nichols, C. A. Pittman, C. Fitzhugh, R. E. Fleming, N. Mohandas, J. F. Tisdale, M. Levine, *J. Vis. Exp.* **2018**, *131*, e56910. <https://doi.org/10.3791/56910>.
- [39] A. Y. Tsibulevskiy, T. K. Dubovaya, B. Z. Sokolinskiy, *Usp. Sovr. Estestvoz.* **2015**, *3*, 151 (in Russian). <https://elibrary.ru/item.asp?id=23945298>.

How to cite this article: T. A. Lomanovskaya, G. A. Piavchenko, V. O. Soldatov, A. A. Venediktov, E. A. Kuzmin, N. L. Kartashkina, S. G. Mukhamedova, T. V. Boronikhina, A. G. Markov, D. V. Telyshev, I. Meglinski, A. N. Yatskovskiy, *J. Biophotonics* **2022**, e202200222. <https://doi.org/10.1002/jbio.202200222>